

Supporting Information

# Balancing Surface Passivation and Catalysis with Integrated $\text{BiVO}_4/(\text{Fe-Ce})\text{O}_x$ Photoanodes in pH 9 Borate Electrolyte

*Lan Zhou,<sup>†, †</sup> Aniketa Shinde,<sup>†, †</sup> Dan Guevarra,<sup>†</sup> Francesca M. Toma,<sup>‡</sup> Helge S. Stein,<sup>†</sup> John M. Gregoire,<sup>†\*</sup> Joel A. Haber<sup>†\*</sup>*

## Corresponding Authors

\*E-mail: [gregoire@caltech.edu](mailto:gregoire@caltech.edu); [jahaber@caltech.edu](mailto:jahaber@caltech.edu).

<sup>†</sup>Joint Center for Artificial Photosynthesis, California Institute of Technology, Pasadena, California 91125 (USA)

<sup>‡</sup>Chemical Sciences Division, Joint Center for Artificial Photosynthesis, Lawrence Berkeley National Laboratory; Berkeley, California 94720 (USA)

## Contents

1. Experimental Details	p S-2
2. Stability characterization	p S-6
3. Comparison of PEC FOMs at pH 13 and pH 9	p S-7
4. Table S1. Tabulated Figures of Merit (FOM) values in pH 9 electrolyte	p S-8

## Experimental Details

A uniform, spin-coated,  $\text{BiVO}_4$  light absorber thin film was deposited onto the fluorine doped tin oxide (FTO) coated side of  $10\text{ cm} \times 10\text{ cm}$  glass plates (TEC-15 Sigma Aldrich) following a literature protocol.<sup>1,2</sup> Solutions of bismuth (III) nitrate pentahydrate (Sigma Aldrich,  $\geq 98\%$ ) in acetylacetone (Sigma Aldrich,  $\geq 99\%$ ) and vanadium(IV)-oxy acetylacetonate in acetylacetone were prepared, mixed, spin-coated onto FTO coated glass plates, and annealed as previously described.<sup>6a</sup> Phase-pure monoclinic  $\text{BiVO}_4$  was verified by X-ray Diffraction (XRD) analysis.

The Fe-Ce oxide libraries were fabricated using reactive RF magnetron co-sputtering of Fe (99.95%, ACI Alloy Inc.) and Ce (99.95%, ACI Alloy Inc.) metal targets at room temperature onto the  $\text{BiVO}_4$ -coated plates. Duplicate Fe-Ce libraries were deposited onto 10 cm-diameter Si wafer with a thermal oxide diffusion barrier to measure film composition and loading. All depositions proceeded in a combinatorial sputtering system (Kurt J. Lesker, CMS24) with  $10^{-5}$  Pa base pressure and a deposition atmosphere composed of inert sputtering gas Ar (0.64 Pa) and reactive gas  $\text{O}_2$  (0.16 Pa). The composition and thickness gradients in each co-sputtered library were attained by positioning the deposition sources in a non-confocal geometry.<sup>11</sup> Prior to deposition, the Fe and Ce targets were pre-cleaned at Ar pressure of 0.80 Pa for 20 min to eliminate possible target contamination. The power applied to both the Ce and Fe targets was 70 W with a deposition time of 30 min. The DC bias voltage on Ce and Fe targets was 236 and 141 V, respectively.

Photoelectrochemical experiments were performed in aqueous 0.1 M boric acid with 0.05 M potassium hydroxide (pH 9). As in our previous work, the same xenon arc lamp combined with a scanning drop electrochemical cell (SDC) were used.<sup>10</sup> Toggled-illumination cyclic voltammetry (CV) measurements were performed on the Fe-Ce libraries with a potential sweep from 1.23 to

0.43 V and back to 1.23 V vs RHE (0 to -0.8 V and back to 0 V vs. the O<sub>2</sub>/H<sub>2</sub>O Nernstian potential) at a scan rate of 0.02 V s<sup>-1</sup>. Illumination was toggled at 0.5 Hz (1.34 s on, 0.67 s off) during the CV. The SDC was rastered along the library with CV measurements acquired every 5 mm, resulting in 339 samples.

**Automated fitting algorithms to extract J-E curves.** Our past work details the automated CV data analysis performed for each sample, resulting in the J-E data shown in Figure 1.<sup>10</sup> Each high throughput cyclic voltammetry (CV) measurement was 80.0 s and swept from 1.23 V to 0.43 V and back to 1.23 V vs. RHE with a sweep rate of 20 mV s<sup>-1</sup>. Illumination was toggled at approximately 0.5 Hz with illumination on for 1.34 s and off for 0.67 s. The voltage and current were acquired every 0.001 V (0.05 s), yielding 27 data points for each illuminated interval and 13 data points for each dark interval.

To capture the quasi-steady state properties of the photoanodes, the performance metrics are calculated from the anodic sweep of the CV using a sigmoidal fitting algorithm. To mitigate the influence of the rapid transient current observed with illumination on/off switching, the first 19 data points and last 3 data points from each illuminated interval, and first 9 data points and last data point from each dark interval are omitted before averaging. The average current from the two nearest dark intervals is subtracted from the average current of each illuminated interval. The dark-subtracted average interval currents are modelled as a four-parameter sigmoid via non-linear least squares fitting, yielding an anodic photocurrent signal,  $J_{photo}$ , as a function of potential for each photoanode sample.

The resulting photocurrent signal,  $J_{photo}$ , is further analyzed to extract  $P_{max}$ ,  $J_{O_2/H_2O}$ ,  $J_{mp}$ ,  $V_{mp}$  and  $V_{OC}$ . Since the  $V_{OC}$  calculation introduces opportunities for systematic errors and sensitivity to experimental noise, the reported values are considered approximate. The primary performance

metrics,  $J_{O_2/H_2O}$  and  $P_{max}$ , are more robustly determined by the high throughput measurement and data processing. Assuming 100% Faradaic efficiency for the OER, the electrochemical power generation  $P_{max}$  was calculated as the product of the reverse bias potential (1.23 V vs RHE – V) and the corresponding photocurrent.

**Transfer efficiency extraction from chopped light illumination.** Charge carrier transfer efficiency can be extracted from analyzing the transient photocurrent response, using a method inspired by Dunn et al.<sup>3</sup> For this analysis, each chopped light illumination CV-curve is split into the respective illumination cycles. For each illumination cycle the signal is reconstructed using an exponential decay and a linear term according to eq. 1. For better fit convergence the data in each illumination cycle is normalized to the peak current and later back transformed.

$$I(t) = I_0 e^{-\tau*(t-t_0)} + m * (t - t_0) + I_2 = I_{transient} + I_{background} + I_{SS} \quad (1)$$

In the CV-curves each illumination period spanned a potential of 27 mV, producing a quasi-steady state current that varies approximately linearly over the illumination period, as opposed to the exponentially decreasing photocurrent transient. By fitting each illumination cycle accordingly, the initial and steady-state photocurrent density were extracted and used to calculate the transfer efficiency for each illumination cycle for all samples according to Eq. 2:

$$\eta_{Transfer} = \frac{I_{SS}}{I_{Initial}} \quad (2)$$

As each illumination cycle spans 40 mV of the CV,  $\eta_{Transfer}$  can only be reported at this interval. The  $\eta_{Transfer}$  at  $E_{mp}$  is reported for the illumination cycle with the closest potential, which is within 20 mV. For illumination cycles where the 20 Hz data recording did not sufficiently capture the initial photocurrent (detected by the first data point after switching on the light being too close to the illumination onset such that the photocurrent continued to grow in the

subsequent data point), the initial photocurrent was obtained by extrapolation a half time step towards the point where illumination commenced (the clocking mismatch was typically one time step).

### Stability characterization

The composition-loading space mapping encompasses the highest performing coatings, and a representative sample ( $\text{Fe}_{0.19}\text{Ce}_{0.81}\text{O}_x$ ,  $0.52 \text{ nmol mm}^{-2}$ ) was chosen for stability characterization, as shown in Figure S1.

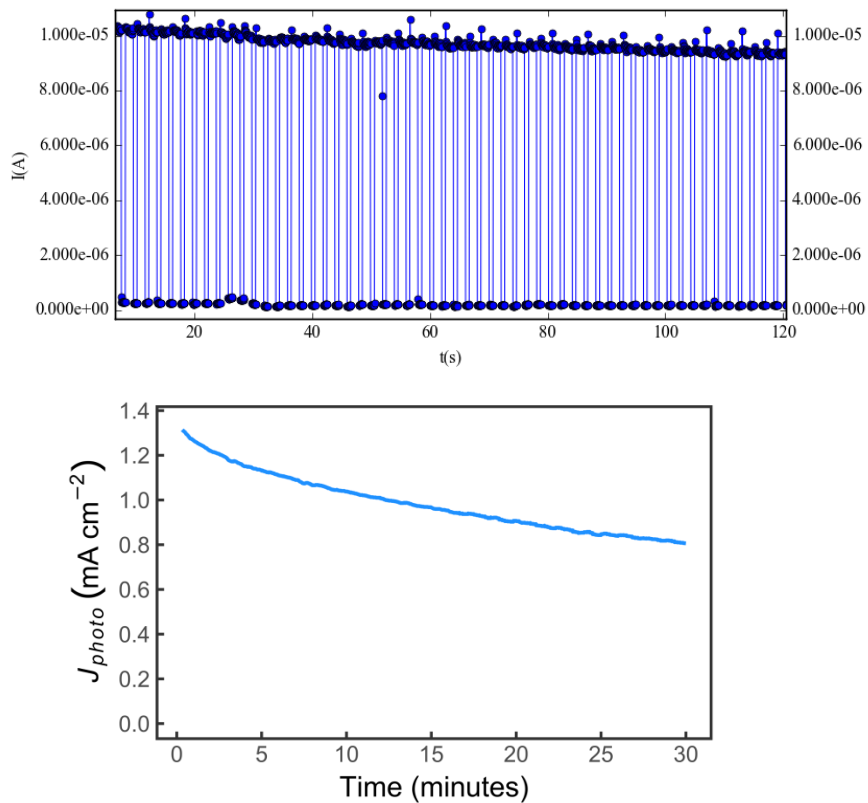


**Figure S1.** Stability evaluation of the  $\text{Fe}_{0.19}\text{Ce}_{0.81}\text{O}_x$  and  $0.52 \text{ nmol mm}^{-2}$  sample using extended toggled illumination CA at 1.23 V vs RHE. Top: First 120 seconds of data collection. Bottom: Photocurrent density over a 30 minute period.

## Comparison of Figures of Merit at pH 13 and pH 9

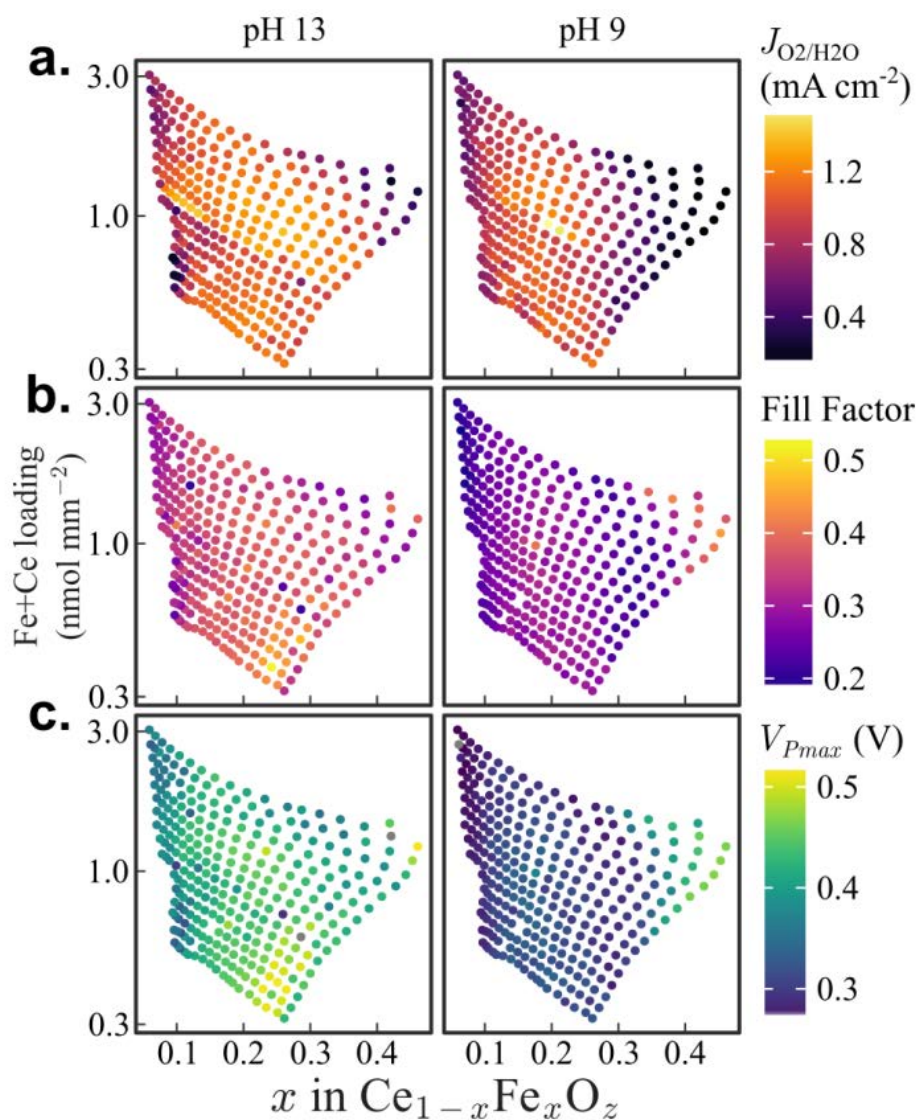


**Figure S2.** Extracted FOMs mapped in the coating composition and loading space for duplicate coating libraries characterized in (left) pH 13 (0.1 M NaOH(aq)) and (right) pH 9 (borate buffer). (a)  $J_{\text{O}_2/\text{H}_2\text{O}}$ , the photocurrent density generated at the Nernstian OER potential, (b) the fill factor, and (c)  $E_{\text{mp}}$ , the potential of the maximum power point for each sample, as extracted from the fitted J-E curves.

**Table S1.** Tabulated Figures of Merit (FOM) values in pH 9 electrolyte used to produce the plots in Figure 2.

sample_ no	frac. Fe	FeCeLoading nmol mm <sup>-2</sup>	P <sub>max</sub> mW cm <sup>-2</sup>	E <sub>mp</sub> V vs RHE	J <sub>O<sub>2</sub>H<sub>2</sub>O</sub> mA cm <sup>-2</sup>	Sigmoid Shape.V	Transfer Eff
20	0.261	0.315	0.262	0.887	1.222	0.090	0.500
21	0.239	0.330	0.248	0.892	1.173	0.084	0.556
22	0.240	0.343	0.225	0.893	1.071	0.089	0.398
23	0.230	0.359	0.174	0.917	0.905	0.097	0.468
24	0.195	0.380	0.233	0.891	1.106	0.092	0.422
25	0.195	0.398	0.244	0.884	1.133	0.091	0.906
26	0.190	0.416	0.269	0.877	1.216	0.087	0.005
27	0.172	0.427	0.226	0.891	1.071	0.094	0.905
28	0.175	0.441	0.200	0.900	0.986	0.100	0.933
29	0.155	0.463	0.156	0.910	0.801	0.105	0.946
30	0.157	0.483	0.192	0.898	0.944	0.105	0.888
31	0.130	0.501	0.249	0.875	1.127	0.091	270.079
32	0.131	0.514	0.217	0.894	1.052	0.103	0.946
33	0.122	0.519	0.180	0.908	0.919	0.108	0.939
34	0.102	0.530	0.140	0.917	0.746	0.112	0.917
35	0.112	0.545	0.141	0.920	0.762	0.115	0.947
36	0.101	0.556	0.115	0.935	0.664	0.118	0.896
37	0.097	0.571	0.119	0.941	0.699	0.116	0.817
39	0.267	0.342	0.233	0.899	1.129	0.089	0.821
40	0.257	0.361	0.177	0.917	0.919	0.096	0.835
41	0.248	0.379	0.214	0.899	1.041	0.089	0.868
42	0.222	0.397	0.234	0.895	1.120	0.086	0.858
43	0.221	0.418	0.258	0.879	1.172	0.086	0.898
44	0.221	0.436	0.266	0.871	1.183	0.084	0.984



45	0.180	0.455	0.277	0.873	1.230	0.084	0.825
46	0.175	0.472	0.261	0.880	1.196	0.090	0.915
47	0.178	0.491	0.212	0.900	1.042	0.094	0.951
48	0.146	0.510	0.194	0.896	0.947	0.101	0.863
49	0.146	0.530	0.197	0.896	0.959	0.102	0.907
50	0.135	0.548	0.246	0.884	1.146	0.096	0.954
52	0.117	0.577	0.188	0.913	0.970	0.103	0.961
53	0.113	0.598	0.137	0.932	0.771	0.110	0.817
54	0.102	0.616	0.143	0.931	0.800	0.109	0.927
55	0.095	0.624	0.132	0.940	0.761	0.110	0.765
56	0.096	0.630	0.113	0.946	0.674	0.114	173.036
58	0.282	0.373	0.245	0.891	1.153	0.080	0.790
59	0.258	0.395	0.208	0.898	0.984	0.087	0.737
60	0.244	0.418	0.235	0.888	1.098	0.086	0.804
61	0.237	0.438	0.230	0.898	1.110	0.084	0.848
62	0.227	0.460	0.252	0.888	1.177	0.083	0.884
63	0.201	0.478	0.214	0.901	1.046	0.091	0.871
64	0.211	0.498	0.215	0.897	1.043	0.092	0.869
65	0.197	0.519	0.268	0.873	1.195	0.085	0.236
66	0.180	0.542	0.248	0.883	1.145	0.088	1.515
67	0.160	0.562	0.248	0.884	1.147	0.091	0.907
68	0.146	0.583	0.238	0.884	1.106	0.095	0.000
69	0.143	0.599	0.237	0.888	1.114	0.094	0.910
70	0.121	0.618	0.239	0.888	1.129	0.096	0.948
71	0.118	0.640	0.208	0.903	1.033	0.100	1.007
72	0.114	0.664	0.152	0.927	0.838	0.111	0.954
73	0.113	0.687	0.158	0.931	0.872	0.106	0.916
74	0.100	0.705	0.142	0.935	0.806	0.107	0.932

75	0.094	0.723	0.117	0.948	0.711	0.117	0.297
77	0.293	0.408	0.110	0.948	0.651	0.122	0.441
78	0.276	0.430	0.171	0.916	0.882	0.092	0.738
79	0.266	0.456	0.198	0.905	0.979	0.086	0.812
80	0.244	0.478	0.238	0.886	1.101	0.080	0.838
81	0.243	0.502	0.243	0.889	1.138	0.084	0.829
82	0.208	0.524	0.231	0.893	1.098	0.086	0.875
83	0.194	0.545	0.254	0.881	1.166	0.089	0.924
84	0.183	0.571	0.263	0.876	1.186	0.087	0.960
85	0.176	0.596	0.249	0.887	1.164	0.089	0.944
86	0.162	0.619	0.234	0.889	1.103	0.093	0.928
88	0.148	0.663	0.204	0.900	1.006	0.099	0.950
89	0.131	0.685	0.161	0.905	0.810	0.103	0.924
90	0.125	0.711	0.216	0.904	1.074	0.098	0.955
91	0.111	0.736	0.209	0.906	1.053	0.103	1.000
92	0.098	0.760	0.181	0.921	0.961	0.102	37.959
93	0.095	0.784	0.154	0.929	0.847	0.106	0.944
96	0.300	0.448	0.094	0.944	0.525	0.118	0.360
97	0.281	0.472	0.120	0.944	0.700	0.111	0.511
98	0.270	0.500	0.182	0.916	0.939	0.092	0.784
99	0.250	0.526	0.234	0.888	1.083	0.080	0.808
100	0.240	0.550	0.235	0.890	1.111	0.086	0.860
101	0.222	0.572	0.224	0.900	1.092	0.090	0.917
102	0.206	0.596	0.210	0.900	1.034	0.095	0.932
103	0.187	0.627	0.247	0.880	1.132	0.089	0.938
104	0.179	0.656	0.269	0.869	1.190	0.086	54.996
105	0.164	0.685	0.256	0.876	1.154	0.089	8.042
106	0.149	0.713	0.242	0.882	1.117	0.092	0.358

107	0.135	0.735	0.209	0.935	0.999	0.095	0.911
108	0.132	0.761	0.214	0.899	1.043	0.095	0.934
109	0.116	0.788	0.186	0.913	0.961	0.099	1.116
110	0.105	0.813	0.190	0.914	0.981	0.101	0.937
111	0.105	0.840	0.177	0.918	0.930	0.102	0.920
112	0.097	0.871	0.166	0.926	0.893	0.100	0.953
115	0.306	0.494	0.078	0.923	0.438	0.140	0.348
116	0.286	0.517	0.060	0.947	0.372	0.167	0.348
117	0.295	0.547	0.155	0.932	0.814	0.089	0.685
118	0.250	0.576	0.170	0.920	0.893	0.093	0.765
119	0.237	0.601	0.181	0.912	0.924	0.091	0.853
120	0.224	0.628	0.204	0.894	0.978	0.088	0.847
121	0.206	0.654	0.233	0.885	1.085	0.086	0.895
122	0.187	0.692	0.238	0.886	1.091	0.087	0.914
123	0.184	0.727	0.265	0.869	1.172	0.085	0.966
124	0.171	0.759	0.265	0.865	1.157	0.088	0.973
125	0.156	0.789	0.240	0.867	1.059	0.089	0.976
126	0.150	0.815	0.249	0.871	1.113	0.093	0.965
127	0.129	0.843	0.224	0.890	1.067	0.097	0.965
128	0.118	0.876	0.177	0.914	0.915	0.102	0.915
129	0.112	0.905	0.189	0.911	0.968	0.102	1.815
130	0.101	0.938	0.171	0.924	0.921	0.104	0.964
131	0.100	0.975	0.134	0.941	0.778	0.110	0.898
134	0.326	0.536	0.074	0.931	0.421	0.141	0.300
135	0.300	0.563	0.091	0.930	0.480	0.109	0.449
136	0.298	0.597	0.122	0.938	0.707	0.116	0.564
137	0.260	0.629	0.169	0.915	0.871	0.091	0.756
138	0.252	0.655	0.190	0.909	0.960	0.091	0.832

139	0.240	0.684	0.182	0.916	0.937	0.091	0.840
140	0.221	0.715	0.201	0.907	1.003	0.092	0.931
141	0.201	0.757	0.225	0.890	1.054	0.064	0.817
142	0.190	0.798	0.262	0.873	1.169	0.084	1.000
143	0.166	0.833	0.258	0.869	1.126	0.086	1.172
144	0.146	0.863	0.250	0.883	1.151	0.092	0.928
145	0.147	0.894	0.240	0.878	1.095	0.094	0.222
146	0.142	0.929	0.205	0.885	0.963	0.099	0.932
147	0.121	0.966	0.200	0.902	0.989	0.100	0.952
148	0.116	1.000	0.184	0.911	0.943	0.101	0.946
149	0.101	1.040	0.150	0.930	0.828	0.106	0.949
150	0.095	1.090	0.130	0.940	0.756	0.111	0.875
151	0.077	1.120	0.128	0.947	0.770	0.113	0.861
152	0.078	1.140	0.108	0.956	0.673	0.116	0.841
153	0.343	0.578	0.054	0.911	0.300	0.148	0.222
154	0.323	0.611	0.086	0.928	0.477	0.113	0.360
155	0.303	0.648	0.122	0.936	0.668	0.112	0.527
156	0.275	0.682	0.129	0.934	0.724	0.106	0.621
157	0.260	0.713	0.177	0.906	0.881	0.087	0.756
158	0.230	0.744	0.205	0.897	0.957	0.080	0.819
159	0.228	0.780	0.189	0.908	0.956	0.096	0.865
160	0.209	0.825	0.200	0.907	1.000	0.091	0.910
161	0.187	0.867	0.192	0.911	0.970	0.092	0.894
162	0.183	0.907	0.251	0.874	1.126	0.087	0.000
163	0.155	0.943	0.234	0.881	1.077	0.091	0.919
164	0.139	0.982	0.236	0.875	1.068	0.092	0.303
165	0.132	1.020	0.231	0.880	1.057	0.094	0.956
166	0.123	1.070	0.179	0.907	0.905	0.101	0.954

167	0.102	1.110	0.167	0.926	0.910	0.107	0.946
168	0.098	1.160	0.135	0.938	0.774	0.112	0.941
169	0.085	1.200	0.124	0.946	0.735	0.111	0.893
170	0.082	1.250	0.113	0.947	0.681	0.115	0.845
171	0.067	1.290	0.097	0.964	0.626	0.114	0.427
172	0.356	0.624	0.048	0.869	0.232	0.152	375.225
173	0.322	0.660	0.076	0.913	0.410	0.126	0.326
174	0.321	0.701	0.098	0.925	0.536	0.115	0.353
175	0.295	0.740	0.130	0.921	0.694	0.103	0.529
176	0.267	0.776	0.174	0.916	0.898	0.093	0.742
177	0.249	0.810	0.237	0.902	1.161	0.085	0.811
178	0.226	0.852	0.285	0.909	1.315	0.086	0.871
179	0.212	0.894	0.340	0.885	1.585	0.089	0.895
180	0.192	0.941	0.345	0.927	1.586	0.097	0.947
181	0.173	0.985	0.304	0.851	1.065	0.090	0.979
182	0.160	1.030	0.264	0.880	1.085	0.081	0.652
183	0.141	1.070	0.279	0.928	1.133	0.105	0.895
184	0.133	1.130	0.252	0.900	1.243	0.101	0.057
185	0.120	1.180	0.232	0.901	1.155	0.105	1.742
186	0.110	1.230	0.198	0.904	0.994	0.104	0.939
187	0.096	1.280	0.167	0.926	0.906	0.104	0.949
188	0.087	1.330	0.124	0.953	0.765	0.111	0.923
189	0.085	1.390	0.104	0.960	0.655	0.109	0.424
190	0.076	1.440	0.101	0.960	0.643	0.116	0.451
191	0.362	0.682	0.030	0.327	0.212	0.306	0.222
192	0.350	0.716	0.055	0.905	0.304	0.151	0.187
193	0.324	0.757	0.085	0.932	0.491	0.129	0.270
194	0.307	0.803	0.081	0.940	0.480	0.133	0.275

195	0.288	0.845	0.171	0.919	0.899	0.095	0.624
196	0.255	0.884	0.202	0.913	1.029	0.090	0.768
197	0.233	0.931	0.235	0.901	1.151	0.087	0.854
198	0.222	0.973	0.233	0.905	1.154	0.089	0.911
199	0.198	1.020	0.299	0.870	1.320	0.083	16.898
200	0.181	1.070	0.267	0.884	1.238	0.089	0.938
201	0.160	1.120	0.266	0.887	1.249	0.093	0.923
202	0.143	1.170	0.273	0.882	1.262	0.094	0.866
203	0.128	1.230	0.234	0.897	1.144	0.100	0.890
204	0.116	1.300	0.219	0.906	1.113	0.108	0.952
205	0.115	1.360	0.183	0.924	0.992	0.107	1.280
206	0.093	1.420	0.151	0.939	0.876	0.111	0.855
207	0.093	1.480	0.126	0.952	0.775	0.114	0.912
208	0.081	1.540	0.095	0.966	0.619	0.115	0.430
209	0.071	1.600	0.067	0.976	0.467	0.120	0.387
210	0.392	0.746	0.012	0.327	0.013	-35.638	0.255
211	0.360	0.783	0.052	0.872	0.251	0.155	283.852
212	0.340	0.824	0.071	0.924	0.411	0.143	0.219
213	0.325	0.874	0.099	0.934	0.565	0.136	0.342
214	0.290	0.921	0.154	0.928	0.840	0.103	0.570
215	0.265	0.963	0.174	0.921	0.923	0.101	0.681
216	0.251	1.010	0.210	0.910	1.064	0.091	0.818
217	0.235	1.060	0.233	0.905	1.156	0.091	0.862
218	0.199	1.120	0.248	0.898	1.205	0.090	0.862
219	0.191	1.180	0.288	0.872	1.285	0.086	0.970
220	0.166	1.230	0.243	0.900	1.185	0.090	1.436
221	0.151	1.290	0.240	0.897	1.159	0.092	0.928
222	0.130	1.360	0.232	0.898	1.131	0.098	0.949

223	0.122	1.430	0.198	0.911	1.020	0.104	0.000
224	0.107	1.500	0.164	0.922	0.880	0.107	0.949
225	0.097	1.570	0.159	0.932	0.891	0.108	0.951
226	0.086	1.630	0.109	0.963	0.698	0.112	0.475
227	0.078	1.710	0.079	0.971	0.533	0.116	0.507
228	0.067	1.780	0.072	0.975	0.494	0.118	0.397
229	0.409	0.820	0.032	0.766	0.108	0.117	0.149
230	0.382	0.856	0.037	0.881	0.203	0.196	0.134
231	0.357	0.900	0.055	0.921	0.316	0.149	0.182
232	0.328	0.952	0.083	0.946	0.504	0.149	0.287
233	0.303	1.000	0.114	0.946	0.678	0.126	0.420
234	0.280	1.060	0.137	0.935	0.774	0.112	0.553
235	0.258	1.110	0.182	0.923	0.974	0.099	0.726
236	0.241	1.170	0.232	0.903	1.144	0.090	0.880
237	0.208	1.230	0.268	0.886	1.249	0.086	0.889
238	0.188	1.290	0.264	0.886	1.229	0.090	0.919
239	0.168	1.350	0.261	0.884	1.214	0.093	0.918
240	0.149	1.420	0.212	0.907	1.064	0.096	0.931
241	0.143	1.490	0.191	0.914	0.989	0.101	0.946
242	0.117	1.580	0.171	0.925	0.925	0.106	0.953
243	0.106	1.660	0.186	0.922	1.000	0.104	0.969
244	0.096	1.740	0.160	0.939	0.927	0.111	0.970
245	0.083	1.810	0.144	0.947	0.855	0.110	0.876
246	0.075	1.890	0.110	0.959	0.706	0.118	0.454
247	0.068	1.970	0.090	0.970	0.611	0.123	0.401
248	0.425	0.888	0.033	0.758	0.110	0.115	0.148
249	0.393	0.925	0.035	0.815	0.141	0.165	0.135
250	0.359	0.967	0.044	0.863	0.209	0.165	0.080

251	0.344	1.020	0.062	0.916	0.353	0.158	0.199
252	0.322	1.080	0.094	0.942	0.555	0.160	0.305
253	0.286	1.140	0.123	0.943	0.708	0.131	0.445
254	0.261	1.210	0.151	0.933	0.840	0.108	0.632
255	0.243	1.270	0.182	0.931	0.993	0.092	0.789
256	0.216	1.330	0.233	0.898	1.127	0.089	0.847
257	0.191	1.400	0.234	0.896	1.130	0.092	0.892
258	0.169	1.480	0.238	0.892	1.136	0.091	0.898
259	0.156	1.550	0.209	0.908	1.053	0.096	1.008
260	0.139	1.640	0.175	0.919	0.921	0.102	0.932
261	0.117	1.730	0.168	0.924	0.905	0.103	0.973
262	0.106	1.810	0.143	0.948	0.846	0.104	0.896
264	0.086	1.990	0.117	0.959	0.738	0.109	0.909
265	0.070	2.090	0.102	0.959	0.642	0.113	0.859
266	0.067	2.180	0.079	0.975	0.555	0.125	0.441
267	0.442	0.972	0.031	0.705	0.091	0.033	0.058
268	0.409	1.040	0.034	0.810	0.134	0.151	0.098
269	0.384	1.100	0.001	1.334	-0.010	-45.227	0.086
270	0.363	1.160	0.050	0.893	0.262	0.162	0.111
271	0.329	1.220	0.070	0.939	0.411	0.145	0.250
272	0.307	1.270	0.108	0.955	0.663	0.129	0.435
273	0.274	1.310	0.130	0.948	0.769	0.107	0.535
274	0.250	1.390	0.175	0.930	0.956	0.094	0.766
275	0.223	1.460	0.224	0.904	1.110	0.091	0.890
276	0.204	1.540	0.222	0.899	1.087	0.094	0.898
277	0.169	1.630	0.217	0.902	1.072	0.093	1.042
278	0.158	1.710	0.190	0.921	1.008	0.098	0.977
279	0.133	1.800	0.193	0.912	0.993	0.101	0.968



280	0.121	1.900	0.168	0.924	0.905	0.104	0.973
281	0.103	2.000	0.150	0.935	0.851	0.109	0.950
282	0.093	2.100	0.107	0.963	0.687	0.112	0.577
283	0.083	2.210	0.107	0.962	0.679	0.110	0.558
284	0.072	2.320	0.082	0.974	0.560	0.115	0.485
285	0.063	2.430	0.039	0.971	0.277	0.140	0.350
286	0.460	1.090	0.033	0.683	0.099	0.035	0.086
287	0.431	1.170	0.035	0.752	0.118	0.073	0.110
288	0.405	1.260	0.035	0.837	0.148	0.127	0.078
289	0.367	1.330	0.044	0.850	0.191	0.124	0.068
290	0.355	1.400	0.052	0.902	0.268	0.133	0.136
291	0.321	1.440	0.079	0.958	0.497	0.122	0.274
292	0.285	1.480	0.108	0.962	0.659	0.106	0.378
293	0.257	1.570	0.158	0.938	0.894	0.098	0.729
294	0.235	1.660	0.189	0.919	0.984	0.093	0.850
295	0.207	1.750	0.201	0.911	1.017	0.091	0.891
296	0.180	1.860	0.181	0.926	0.971	0.098	0.889
297	0.157	1.960	0.197	0.910	0.997	0.095	44.680
298	0.136	2.080	0.184	0.908	0.936	0.101	0.950
299	0.121	2.190	0.169	0.922	0.901	0.103	0.975
300	0.105	2.300	0.146	0.936	0.820	0.102	0.976
301	0.088	2.420	0.104	0.962	0.662	0.110	0.624
302	0.077	2.540	0.105	0.962	0.669	0.112	0.496
303	0.067	2.630	0.087	0.974	0.593	0.117	0.936
304	0.061	2.700	0.097	0.975	0.669	0.115	0.497
305	0.461	1.210	0.033	0.714	0.104	0.085	0.105
306	0.430	1.320	0.033	0.673	0.101	0.046	0.128
307	0.395	1.420	0.037	0.743	0.124	0.044	0.013

308	0.361	1.500	0.040	0.765	0.139	0.053	0.060
309	0.334	1.570	0.001	1.334	-0.013	-29.686	0.097
310	0.294	1.620	0.056	0.935	0.331	0.133	0.183
311	0.265	1.650	0.079	0.964	0.509	0.119	0.295
312	0.235	1.760	0.116	0.961	0.731	0.109	0.505
313	0.205	1.860	0.155	0.931	0.854	0.098	0.753
314	0.175	1.960	0.161	0.932	0.885	0.098	0.851
315	0.161	2.080	0.161	0.932	0.883	0.096	0.903
316	0.141	2.210	0.170	0.923	0.903	0.098	161.015
317	0.122	2.340	0.155	0.926	0.843	0.103	0.945
318	0.108	2.480	0.122	0.951	0.730	0.105	0.878
319	0.088	2.610	0.106	0.959	0.663	0.108	217.451
320	0.077	2.740	0.098	0.961	0.619	0.110	0.458
321	0.070	2.890	0.077	0.970	0.516	0.117	0.656
322	0.059	3.030	0.079	0.972	0.543	0.124	0.955
325	0.419	1.460	0.037	0.839	0.154	0.118	0.063

## References

- (1) Cooper, J. K.; Gul, S.; Toma, F. M.; Chen, L.; Liu, Y. S.; Guo, J. H.; Ager, J. W.; Yano, J.; Sharp, I. D. Indirect Bandgap and Optical Properties of Monoclinic Bismuth Vanadate. *J. Phys. Chem. C* **2015**, *119*, 2969.
- (2) Jeon, T. H.; Choi, W.; Park, H. Cobalt-Phosphate Complexes Catalyze the Photoelectrochemical Water Oxidation of BiVO<sub>4</sub> Electrodes. *Phys. Chem. Chem. Phys.* **2011**, *13*, 21392.
- (3) Dunn, H. K.; Feckl, J. M.; Muller, A.; Fattakhova-Rohlfing, D.; Morehead, S. G.; Roos, J.; Peter, L. M.; Scheu, C.; Bein, T. Tin Doping Speeds Up Hole Transfer During Light-Driven Water Oxidation at Hematite Photoanodes. *Phys. Chem. Chem. Phys.* **2014**, *16*, 24610.